Journal of Applied Mechanics and Technical Physics, Vol. 41, No. 4, 2000

STRENGTH OF WATER UNDER PULSED LOADING

A. A. Bogach and A. V. Utkin

UDC 532.538+539.539

Experiments were performed to study the strength of water under conditions of pulsed extension, which is typical of the interaction between a triangular compression pulse and a free surface. The tests were performed in a wide (40–1000 MPa) *range of variation in the amplitude of the compression pulse at deformation rates of* 10^4–10^5 $\sec^{-1}$. *It is found that as the compression-pulse amplitude increases from* 150 *to* 1050 MPa, *the strength of water decreases from* 46 *to* 22 MPa. *The deformation rate was found to have little effect on the strength. The possibility of using the model of homogeneous nucleation (formation of cavitation nuclei) to interpret the data obtained is discussed.*

According to theoretical concepts, liquids can sustain considerable tensile stresses reaching 100–1000 MPa [1–3]. At the same time, much smaller values were obtained in static tests (see [4]) and in cavitation studies in an intense acoustic field [5–7]. This discrepancy is due to the fact that in real liquids, the presence of heterogeneous sites (interfaces, solid inclusions, gas bubbles, etc.) gives rise to pore growth, which leads to fracture of the liquids. In water, for example, the total amount of heterogeneities with characteristic dimensions of 0.001–10 μm is 10^5–10^6 cm^{-3} [8, 9]. Of all the impurities in the liquid, only bubbles in the bulk and in small cracks of undiluted particles can have a considerable effect on its strength [7].

The strength of the liquid under dynamic loading is closer to the theoretical value. In the present study, for dynamic extension of the liquid, we use spalling phenomena that occur in the reflection of compression pulses from the free surface of the substance to be examined [10]. The advantage of this approach is that the fracture caused by 1-μsec pulses is volume (the effect of the boundaries is negligible) and occurs in a thin layer of the substance. This leads to a decreased number of heterogeneous sites that can influence the fracture of the liquid. Moreover, the precompression in the shock wave is likely to result in the collapse of the pores, which also intensifies homogeneous nucleation.

The pulsed extension of liquids under shock-wave loading was used to study the cavitation of glycerin [11–13], water [14–16], ethylene glycol [15], ethanol [16], and mercury [17]. Glycerin is most extensively studied, for which a relation between the spall strength and the temperature was determined [13] and it was shown that at 20°C, its strength is equal to 60 MPa for any deformation rate [12]. The values of the spall fracture of water obtained by different authors differ by several orders (from 3.9 MPa [15] to 400 MPa [18]). There are no reliable experimental data on how the deformation conditions influence the character of fracture. At the same time, the phenomenon of cavitation is of considerable practical interest, which stimulates the study of the behavior of water upon pulsed extension. In this paper, the results of experimental determination of the spall strength of water are given for wide ranges of compression-pulse amplitudes and durations and the question as to whether the homogeneous-nucleation model can be used to interpret the results obtained is considered.

Institute of Chemical Physics, Russian Academy of Sciences, Chernogolovka 142432. Translated from Prikladnaya Mekhanika i Tekhnicheskaya Fizika, Vol. 41, No. 4, pp. 198–205, July–August, 2000. Original article submitted June 9, 1999; revision submitted August 3, 1999.

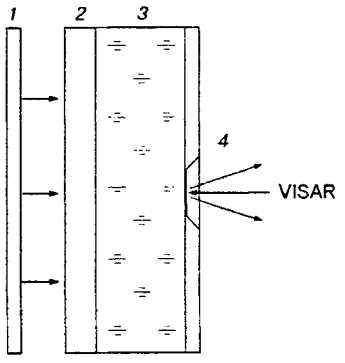

Fig. 1

TABLE 1

Test No.	h_w, mm	P_0, MPa	W_0, m/sec	ΔW, m/sec	P_s, MPa	$\dot{\varepsilon} \cdot 10^{-4}$, sec^{-1}
1	8	310	206	—	—	9
2	8	310	413	56 ± 2	42.0 ± 1.5	9
3	8	300	403	55 ± 2	41.0 ± 1.5	5
4	8	40	52	> 50	> 38	2.7
5	8	150	200	62 ± 5	46.0 ± 4.0	5
6	2	406	542	59 ± 2	44.0 ± 1.5	14
7	4	430	574	52 ± 2	39.0 ± 1.5	10
8	8	1050	1403	30 ± 2	22.5 ± 2.0	2

Experimental Results. A scheme for experimental studies of the pulsed extension of water is shown in Fig. 1. Shock waves were generated as a result of the collision of the aluminum striker 1 of thickness 0.2–0.4 mm and diameter 60 mm, which is accelerated by an explosive thrower [10] to velocities of 200–600 m/sec, against the acrylic plastic bottom of a dish (screen 2) 2 mm thick. The loading conditions were varied by changing the size of the explosive charge, the thickness of the striker, and the thickness h_w of water layer 3 (see Table 1). To record the velocity, we used a VISAR laser interferometer [19] with an interferometer constant equal to 80.8 m/sec; the measurement error was ±2 m/sec and the temporal resolution was approximately 5 nsec. The laser beam was reflected from the aluminum foil 4 (7 μm thick), which separated water from air. The geometrical parameters of the setup ensured the one-dimensional loading conditions and excluded the arrival of the lateral unloading wave during the experiment. Figure 2a and b shows the mass-velocity profiles plotted with the use of experimental data. The figures at the curves correspond to the experiment number. The velocity profiles are arbitrarily shifted along the t axis relative to each other, since the zero time is of no significance. In all the tests (except for test No. 3 where fresh tap water was used), distilled water at an initial temperature of 20°C was used. On reaching the free surface, the compression pulse was triangular, which was determined in the experiments performed according to a scheme similar to that shown in Fig. 1, but the foil was placed into water in this case. As an example, Fig. 2a shows the mass-velocity profile which refers to test No. 1, where the foil was placed inside a thick layer of water 8 mm from the screen.

Upon reaching the free surface, the shock wave gives rise to a jump in the surface velocity up to a W_0 value (see Table 1) equal to the double mass velocity in the shock wave. A centered rarefaction wave propagates deep into the water and interacts with the incident unloading wave; this leads to internal fracture, i.e., spalling. During the fracture, the tensile stresses relax to zero and form a compression wave, which arrives at the free surface in the form of a so-called spalling pulse. Subsequent velocity oscillations are caused by circulation of the waves between the specimen surface and the fracture region. These specific features are observed for the velocity profiles that refer to test Nos. 2 and 3 (see Fig. 2a). A comparison of profiles 1 and 2 shows that the rule of velocity doubling is fulfilled with good accuracy. This supports the absence of cavitation at the foil–water interface, which otherwise leads to weaker adhesion between the foil and water and, as a sequence, to a smaller steepness of the velocity drop immediately after the shock wave has reached the free surface. The value of the spall strength P_s, which characterizes the maximum tensile stresses in the specimen, was determined from the minimum velocity W_m attained in front of the spalling pulse [10]: $P_s = 0.5\rho_0 c_0 \Delta W$, where $\Delta W = W_0 - W_m$ and ρ_0 and c_0 are, respectively, the initial density and velocity of sound in water at 20°C and at a pressure of 10^5 Pa.

Figure 2 shows the free-surface velocity of water W versus time t for the case where the amplitude of the compression pulse P_0 increases from 40 to 1000 MPa and the deformation rate in the unloading part of the pulse $\dot{\varepsilon} = (dW/dt)/(2c_0)$ increases from 10^4 to 10^5 sec^{-1}. The strength P_s, calculated by the above formula, is given in Table 1. It is seen that the experimental results are characterized by good reproducibility and an

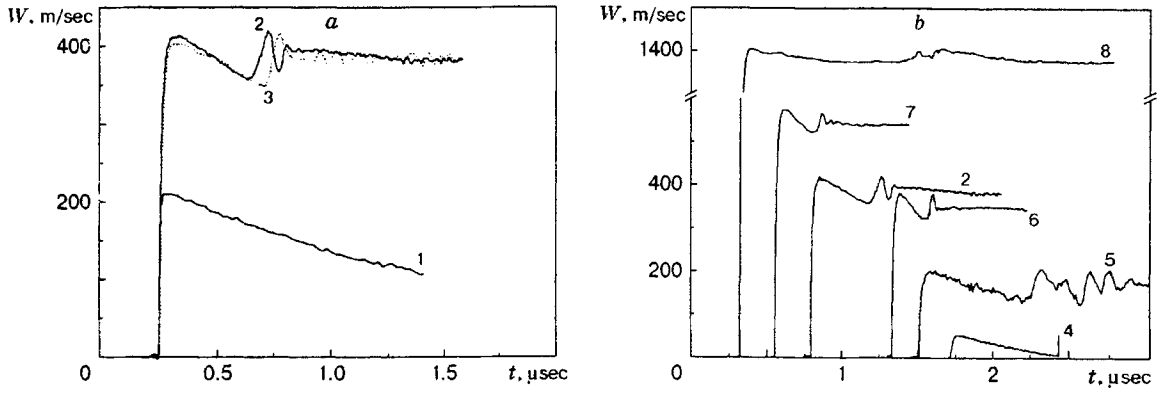

Fig. 2

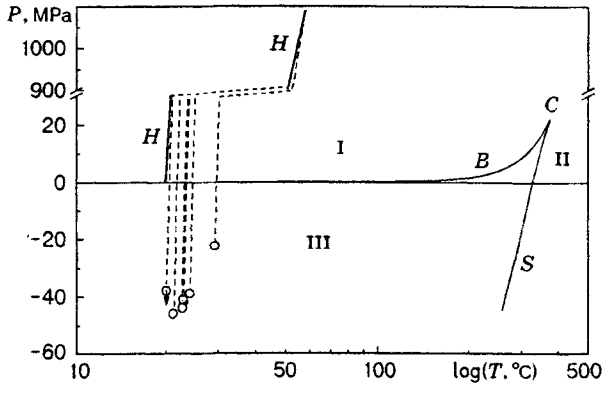

Fig. 3

almost constant value of P_s in the entire interval of deformation rates, and the strength of fresh tap water (test No. 3) is equal to that of distilled water. An exception is test No. 8, in which the shock-wave amplitude is maximum and loading was performed by a plane-wave generator through a steel screen rather than by the striker. In this test, the deformation rate was almost the same as in test No. 4, and the compression-wave amplitude was a factor 25 greater than in test No. 4, which results in a twofold decrease in the spall strength. We emphasize that, in fact, the tensile stresses in test No. 4 slightly exceed the measured value of 38 MPa, since the minimum velocity recorded is due to the fact that not the spall pulse but the second shock wave formed after the collision of the massive steel attenuator following the striker against the water reached the free surface.

We point out some specific features of the free-surface velocity profiles. First, the front of the spalling pulse is very steep, which shows that the porosity growth rate in the cavitation region is high after the onset of fracture [20]. Second, the periodic velocity oscillations in the spall plate are not noticeable in contrast, for example, to metals where these oscillations are pronounced, probably owing to the fact that the cavitation region enlarges with time and approaches the free surface. The boundary between the water and the fracture region is not distinct, which also leads to smoothed oscillations. Utkin [21] considered the problem of viscous fracture of a medium under spalling conditions and showed that for instantaneous fracture, the spalling-pulse amplitude is equal to the incident-wave amplitude and it is smaller in other cases. In the resulting profiles, the spalling-pulse amplitude is equal to the maximum velocity: it exceeds this value in test No. 3, the difference being greater than the experimental error. This is probably due to the fact that the motion of the cavitation-region boundary influences the formation of a spalling pulse.

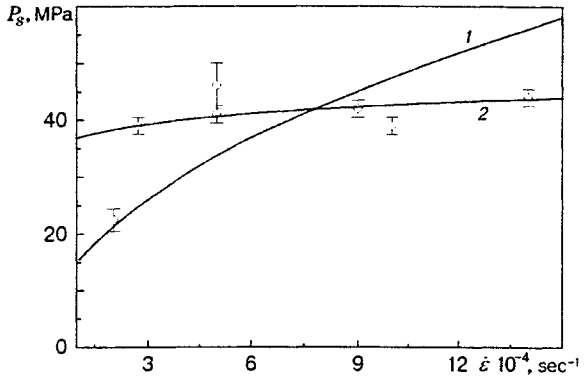

Fig. 4

Discussion of Experimental Results. The spall fracture of liquids differs fundamentally from that of metals, polymers, and other condensed media. For pulsed extension-induced negative pressures, the liquid is in the region of metastable state III (Fig. 3), whose lifetime depends on the purity of the liquid and extension conditions. Figure 3 shows the phase plane of water in the neighborhood of the two-phase water I–steam II region (P [MPa] is the pressure and T [°C] is the temperature). The liquid spinodal S and the phase-equilibrium curve (binodal) B plotted with the use of the data of [4] and [22], respectively, bound the metastability region; C is the critical point.

In the experiments, water was compressed along the Hugoniot curve H up to the maximum pressure P_0 (see Table 1) and then unloaded isentropically to the states shown by light circles in Fig. 3. The arrow indicates that the strength value measured in test No. 4 gives the lower bound. The Hugoniot curve H and unloading isentropic curves (dashed curves in Fig. 3) were calculated with the use of shock-compression data from [23] and the caloric equation of state of water given in [24]. The metastable state fails as a result of the growth of pores, which always exist in the liquid and are generated by thermal fluctuation processes. We now consider the effect of homogeneous and heterogeneous nucleation on cavitation under spalling conditions.

Let the strength observed in the experiments be due to the growth of pores that exist in the liquid. With allowance for viscosity, the variation in porosity $V_p = (4/3)N\pi R^3$ is described by the equation [25]

$$\dot{V}_p = 4N\pi R^2\dot{R} = -4N\pi R^2 RP/(4\eta) = -3V_pP/(4\eta), \tag{1}$$

where R is the radius of the pore, N is the number of pores per unit volume, and η is the viscosity of water. The dot denotes differentiation with respect to time.

An analysis of the effect of the kinetics of pore growth on the dynamics of the wave interaction upon spalling [26] shows that a minimum in the free-surface velocity profile forms when $\dot{V}_p$ exceeds the critical value proportional to the deformation rate in the unloading part of the incident pulse $\dot{\varepsilon}$: $\dot{V}_p = \gamma\dot{\varepsilon}$, where $\gamma \sim 1$. If it is assumed that the bubble density is $N \sim 10^3$–10^4 cm^{-3} for $R_0 = 1.5$ μm [9] under normal conditions ($P \approx 10^5$ Pa and $T = 20$°C), we find that at zero time the value of the rate $\dot{V}_p$ is of the order of 10^5 sec^{-1}, which coincides with the deformation rate in the experiment. Therefore, using the heterogeneous-nucleation model, one can obtain spall-strength values close to the experimental values. However, one should keep in mind that the extension is preceded by shock-wave compression and water is subjected to a pressure equal to the incident-wave amplitude for approximately 0.5 μsec. As a result, the pores partially collapse, the effect of heterogeneous nucleation on cavitation becomes weak, and the effect of homogeneous nucleation becomes more pronounced under spalling conditions. This is supported by the coincidence of the experimental values of the spall strengths of distilled and fresh tap water. Moreover, it follows from the kinetic equation (1) that $P_s \sim \sqrt{\dot{\varepsilon}}$ [26]. One can see that the character of this dependence (curve 1 in Fig. 4) does not agree with the experimental results.

We consider the effect of homogeneous nucleation on the pore growth upon spalling. According to the thermodynamic theory of fluctuations [1, 25], the number of pores J with the critical radius $R_c = 2\sigma/P_s$ (σ is the surface-tension coefficient) which form per unit volume in a unit time is given by

$$J = N_0 \frac{\sigma}{\eta} \sqrt{\frac{\sigma}{kT}} \exp\Big(-\frac{16\pi\sigma^3}{3P_s^2 kT}\Big). \tag{2}$$

where N_0 is the number of molecules per unit volume of the liquid. T [K] is the temperature, and k is the Boltzmann constant. Using relations (2), Zel'dovich showed [1] that for water, the ultimate strength J is approximately 200 MPa. As was noted above, the ultimate strength upon spalling is determined from the minimum in the free-surface velocity profile, which in turn forms when the porosity growth rate exceeds the critical value.

The kinetic equation (1) is replaced by the system of two equations

$$\dot{V}_p = \frac{4}{3}\pi R_c^3 J + \int_0^t 4\pi R^2 \dot{R} J\, dt \approx \frac{4}{3}\pi R^3 J, \tag{3}$$

$$\dot{R} = -(PR + 2\sigma)/\eta. \tag{4}$$

The first and second terms on the right side of (3) allow for the increase in porosity owing to homogeneous nucleation and pore growth, respectively. Simplification of Eq. (3) is a result of the assumption of small variation in J in the formation of a spalling pulse. In contrast to (1), relation (4) also takes into account the effect of surface-tension forces on the kinetics of pore growth for $R \sim R_c$. Since the derivative $\dot{R} \to R_c$ vanishes as $\dot{R}$ (the nucleus is in an equilibrium but unstable state), the integration in (4) should be performed from the point $R' = R_c + \Delta R$, where $\Delta R = \sqrt{3kT/(8\pi\sigma)}$. One should also keep in mind that, for small $R \sim 10$ nm, the surface tension decreases linearly with the pore radius [4]. This leads to an exponential increase in the nucleation rate. For example, if σ decreases by threefold for $R = R_c$, the characteristic value of J is of the order of $10^{\cdots}$ $\mathrm{m}^{-3}\cdot\mathrm{sec}^{-1}$. Even in this case, the initial porosity growth rate is small (approximately 10 sec^{-1}); nevertheless, a minimum forms in the free-surface velocity profile, since $\dot{V}_p$ increases with time [26]. The minimum is expected to be fairly smooth, which is observed in the experiments.

Assuming that precisely the nucleation process is responsible for the increase in porosity rather than the subsequent pore growth in a viscous liquid, we determine, from Eqs. (2) and (3), the character of the relation between the spall strength and the deformation rate [26]:

$$P_s \approx A/\sqrt{\ln(B/\dot{\varepsilon})}, \tag{5}$$

where A and B are constants which depend on the temperature both explicitly and in terms of the viscosity and the surface-tension coefficient. The lower bound of B is estimated to be of the order of 10^{15} sec^{-1}.

Curve 2 in Fig. 4 is plotted by relation (5) for $A = 110$ MPa and $B = 10^{16}$ sec^{-1}. One can see that relation (5) agrees with the experimental data (points in Fig. 4). Test No. 8 with the maximum amplitude of the shock wave is an exception. In this case, the abrupt decrease in the strength cannot be explained only by the increase in the average temperature after unloading, since it is only 10°C greater than that in test No. 4 with the minimum shock-wave amplitude (see Fig. 3), which leads to a decrease in the constant A by approximately 10% and not by 40%, which is necessary for agreement with the experiment. It is likely that the effect of the shock wave is not limited by the pore collapse and the change in the average temperature after unloading.

Heating of the liquid can be significant in the neighborhood of a deformed pore. This causes the formation of "hot spots" whose dimensions are close to the initial diameter of the cavity, and the temperature of micron pores can reach 1000°C [5]. The temperature in the site decreases abruptly with time, and the dimension of the elevated-temperature region increases as a square root of the time. Therefore, at the moment the tensile stresses occur in the liquid, micron regions with a temperature higher than the residual temperature, in which the homogeneous nucleation proceeds at the highest rate, can exist. Our consideration

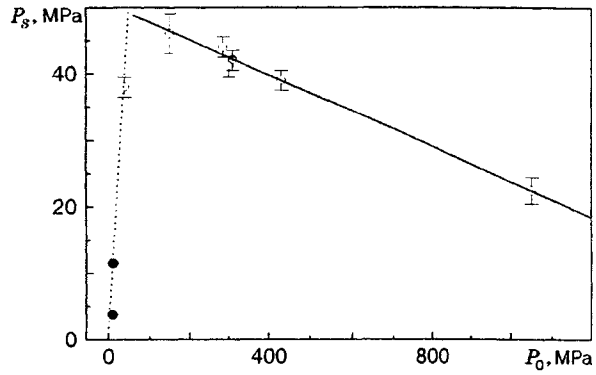

Fig. 5

is consistent with test No. 8 if the temperature in these regions is assumed to be approximately 60°C greater than the average temperature. Moreover, the strength is bound to decrease noticeably with increase in the shock-wave amplitude, since not only the residual temperature but also the "hot spot" temperature increases in this case. This is supported by the experimental results given in Fig. 5, where the solid curve refers to the linear approximation of our experimental data (open points). For given deformation rate and initial temperature, there exists a compression-pulse amplitude at which the spall strength is maximum. With further decrease in pressure, the cavitation still occurs, but the tensile stresses do not exceed the compression-pulse amplitude, which is precisely the estimate of strength of the liquid (the dotted curve in Fig. 5). This probably explains the low spall strength measured by Marston and Urgen [15] (filled points in Fig. 5).

Thus, an analysis of the spall-strength data for water shows that the homogeneous-nucleation model describes the experimentally observed weak dependence of the strength on the deformation rate. The decrease in the tensile stresses induced by the increase in the compression-pulse amplitude is also explained within the framework of this approach if the elevated-temperature regions are assumed to occur as a result of the collapse of pores, which always exist in the liquid.

REFERENCES

1. Ya. B. Zel'dovich, "Theory of occurrence of the new phase. Cavitation," *Zh. Éksp. Teor. Fiz.*, **12**, Nos. 11/12, 525–538 (1942).
2. J. C. Fisher, "The fracture of liquids," *J. Appl. Phys.*, **19**, 1062–1067 (1948).
3. M. Kornfel'd, *Elasticity and Strength of Liquids* [in Russian], Gostekhteoretizdat, Moscow–Leningrad (1951).
4. V. P. Skripov, *Metastable Liquids* [in Russian], Nauka, Moscow (1972).
5. G. Flynn, "Physics of acoustic cavitation in a liquid," in: W. Mason (ed.), *Physical Acoustics*, Vol. 1: *Methods and Devices for Ultrasonic Investigations* [Russian translation], Mir, Moscow (1967), pp. 7–138.
6. N. A. Roi, "Occurrence and regimes of ultrasonic cavitation (Review)," *Akust. Zh.*, **3**, No. 1, 3–21 (1957).
7. M. G. Sirotyuk, "Experimental study of ultrasonic cavitation," in: *Physics and Technology of Strong Ultrasound. Strong Ultrasonic Fields* [in Russian], Nauka, Moscow (1968), pp. 167–220.
8. V. K. Kedrinskii, "Nonlinear problems of cavitation fracture of liquids under explosive loading (Review)," *Prikl. Mekh. Tekh. Fiz.*, **34**, No. 3, 74–91 (1993).
9. V. K. Kedrinskii, A. S. Besov, and I. É. Gutnik, "Inversion of the two-phase state of a liquid under pulsed loading," *Dokl. Ross. Akad. Nauk*, **352**, No. 4, 477–479 (1997).
10. G. I. Kanel', S. V. Razorenov, A. V. Utkin, and V. E. Fortov, *Shock-Wave Phenomena in Condensed Media* [in Russian], Yanus-K, Moscow (1996).
11. D. C. Erlich, D. C. Wooten, and R. C. Crewdson, "Dynamic tensile failure of glycerol," *J. Appl. Phys.*, **42**, No. 13, 5495–5502 (1971).

12. G. A. Carlson and K. W. Henry, "Technique for studying dynamic tensile in liquids: Application to glycerol," *J. Appl. Phys.*, **44**, No. 5, P. 2201–2206 (1973).
13. G. A. Carlson and H. S. Levine, "Dynamic tensile strength of glycerol," *J. Appl. Phys.*, **46**, No. 4, 1594–1601 (1975).
14. P. L. Marston and G. L. Pullen, "Cavitation in water induced by the reflection of shock waves," in: *Proc. of the Conf. of the Amer. Phys. Soc. on Shock Waves in Condensed Matter* (Menlo Park, CA, 23–25 June, 1981), AIP, New York (1982), pp. 515–519.
15. P. L. Marston and B. T. Urgen, "Rapid cavitation induced by the reflection of shock waves," in: *Proc. of the Conf. of the Amer. Phys. Soc. on Shock Waves in Condensed Matter* (Spokane, Washington, 22–25 July, 1985), Plenum Press, New York (1986), pp. 401–405.
16. A. N. Dremin, G. I. Kanel', and S. A. Koldunov, "Analysis of the spall in water, ethanol, and acrylic plastic," in: *Proc. III All-Union Symp. on Combustion and Explosion* (Leningrad, July 5–10, 1971), Nauka, Moscow (1972), pp. 569–574.
17. G. A. Carlson, "Dynamic tensile strength of mercury," *J. Appl. Phys.*, **46**, No. 9, 4069–4070 (1975).
18. A. P. Rybakov, *Mechanics of Spall Fracture* [in Russian], Izd. Perm. Vysh. Voen. Komandno-Inzh. Uch., Perm' (199[illegible]
19. J. R. Asay and L. M. Barker, "Interferometric measurement of shock-induced internal particle velocity and spatial variations of particle velocity," *J. Appl. Phys.*, **45**, No. 6, 2540–2546 (1974).
20. A. V. Utkin, "The effect of the initial fracture rate on the formation of a spalling pulse," *Prikl. Mekh. Tekh. Fiz.*, **34**, No. 4, 140–146 (1993).
21. A. V. Utkin, "The effect of the fracture rate on the dynamics of a shock-loading pulse–body surface interaction," *Prikl. Mekh. Tekh. Fiz.*, **33**, No. 6, 82–89 (1992).
22. M. P. Vukalovich, *Tables of Thermodynamic Properties of Water and Steam* [in Russian], Énergiya, Moscow–Leningrad (1965).
23. K. P. Stanyukovich (ed.), *Physics of Explosion* [in Russian], Nauka, Moscow (1975).
24. W. A. Walker and M. M. Sternberg, "The Chapman–Jouguet isentrope and the underwater shockwave performance of pentolite," in: *Proc. of the 4th Int. Symp. on Detonation* (White Oak, October 12–15, 1965), Office of Naval Res.-Dept. of the Navy, Washington (1967), pp. 23–29.
25. Yu. M. Kagan, "Kinetics of boiling of a pure liquid," *Zh. Fiz. Khim.*, **34**, No. 1, 92–101 (1960).
26. A. V. Utkin, "Determination of the constants of spall-fracture kinetics of materials using experimental data," *Prikl. Mekh. Tekh. Fiz.*, **38**, No. 6, 157–167 (1997).